



HAL
open science

Chemical Vapor Deposition and Characterization of Thick Silicon Carbide Tubes for Nuclear Applications

P. Drieux, G. Chollon, A. Allemand, Sylvain Jacques

► To cite this version:

P. Drieux, G. Chollon, A. Allemand, Sylvain Jacques. Chemical Vapor Deposition and Characterization of Thick Silicon Carbide Tubes for Nuclear Applications. Processing and Properties of Advanced Ceramics and Composites V: Ceramic Transactions, Volume 240, pp.87-98, 2013, <10.1002/9781118744109.ch10>. <hal-02979857>

HAL Id: hal-02979857

<https://hal.science/hal-02979857v1>

Submitted on 27 Oct 2020

HAL is a multi-disciplinary open access archive for the deposit and dissemination of scientific research documents, whether they are published or not. The documents may come from teaching and research institutions in France or abroad, or from public or private research centers.

L'archive ouverte pluridisciplinaire **HAL**, est destinée au dépôt et à la diffusion de documents scientifiques de niveau recherche, publiés ou non, émanant des établissements d'enseignement et de recherche français ou étrangers, des laboratoires publics ou privés.



HAL Authorization

CHEMICAL VAPOR DEPOSITION AND CHARACTERIZATION OF THICK SILICON CARBIDE TUBES FOR NUCLEAR APPLICATIONS

P. Drieux^{1,2}, G. Chollon¹, A. Allemand², S. Jacques¹

¹Laboratoire des Composites ThermoStructuraux, CNRS, Herakles, CEA, Université
Bordeaux 1

²CEA Le Ripault
FRANCE

ABSTRACT

SiC/SiC composites have an outstanding mechanical behavior under irradiation, but their high porosity excludes their use as nuclear fuel claddings in the future nuclear power plants. A complementary thick and tight SiC sheath could be a solution to ensure the first barrier towards fissile materials.

The aim of this work is to make long, free standing and high strength SiC tubes. A few hundred micrometers thick tubular coatings were produced by chemical vapor deposition at atmospheric pressure, from CH₃SiHCl₂/Ar/H₂ mixtures. Their chemical compositions and microstructures were studied by electron probe microanalysis, Raman spectroscopy and scanning electron microscopy.

The deposition rate, composition and microstructure were investigated as a function of the substrate temperature and the gas flow rates. A Fourier transformed infrared spectroscopy analysis of the gas phase was carried out at the reactor outlet. The Si/C ratio, the SiC degree of crystallization and the surface morphology are strongly related to the maturation of the gas phase and the deposition regime.

INTRODUCTION

The structural components of a nuclear fusion or fission reactor must show a low induced radioactivity after neutron irradiation. Tubular SiC/SiC composites [1, 2] are materials of prime interest to be part of the nuclear fuel claddings of future power plants [3] thanks to their low neutron activation characteristics [4], but also their high strength and fracture toughness at high temperature [5].

The optimization of SiC/SiC composites for nuclear purposes requires high thermal properties as well as excellent gas impermeability [6]. The latter point has led to the idea of covering the composite with a dense and impermeable SiC_β sheath having high mechanical properties and stability at high temperature and under neutron irradiation [7].

Well known exemplary SiC coating materials, in terms of mechanical properties, are SiC monofilaments [8]. They are prepared by chemical vapor deposition at atmospheric pressure (APCVD) on a hot filament substrate, using chlorosilanes (e.g. dichloromethylsilane: DCMS) diluted in hydrogen as the SiC precursor [9]. A failure strength up to 6 GPa and a strain of about 1.5 % can indeed be reached in the high performance SCS-Ultra from Specialty Materials Inc. The aim of the present study is to prepare SiC tubes by APCVD, with a composition, microstructure and morphology compatible with high strength and strain at failure.

The present paper reports on our latest results on the elaboration and characterization of thick SiC tubular coatings. Efforts have been mainly concentrated on the adjustment of the stoichiometry and the microstructure of the SiC deposit. The influence of the deposition temperature, the initial composition of the gas mixture and the total flow rate on the physical

and chemical properties and growth kinetics of the coatings have been investigated. Fourier transform infrared (FTIR) analyses of the gas phase at the reactor outlet have also been performed to follow the decomposition of the precursor.

EXPERIMENTAL APPROACH

CVD process

The laboratory-scale reactor for the APCVD of thick tubular SiC coatings is presented in Fig. 1. It consists of a horizontal silica glass tube ($L = 1000$ mm, $\varnothing_{\text{int}} = 46$ mm) connected to gas inlet/outlet flanges at both ends. Tubular SiC deposits can be obtained by two ways: an outer coating on a solid graphite substrate or an inner coating inside a silica tube.

In reference to the filaments process, a graphite solid cylinder ($L = 200$ mm, $\varnothing_{\text{ext}} = 10$ mm) was first used as a substrate. In this case, the CVD reactor operated in a cold-wall configuration, since the substrate was directly heated by induction, while the external silica chamber remained relatively cold. The first experiments led to a main difficulty related to the cold-wall configuration and the horizontal position of the cylinder: a thickness gradient was indeed observed between the upper and lower parts of the rod, due to the convection of the gases. Furthermore, the removal of the graphite substrate is difficult and the final morphology of the SiC coating is strongly affected by the roughness and the porosity of the graphite substrate. The inside of a silica tube ($L = 500$ mm, $\varnothing_{\text{int}} = 8$ mm) was used as an alternative substrate, the gases being forced to flow through it. The silica tube was brought to high temperature by a surrounding graphite susceptor heated by induction. This unit is placed inside the original 46 mm diameter silica tube. This new reactor was then in a hot-wall configuration, since the whole 8 mm diameter reaction chamber, including the substrate walls, was isothermal in the hot deposition area (4 cm).

Dichloromethylsilane ($\text{H}_3\text{CSiHCl}_2$, DCMS) was used as the SiC precursor [9]. The DCMS vapor saturation was obtained from a H_2 carrier gas going through a bubbler maintained at 20°C ($P_{\text{DCMS}} = 48$ kPa). The DCMS concentration was adjusted by further diluting the initial saturated DCMS/ H_2 mixture in a secondary H_2 flow.

As the final aim of this work is the manufacturing of relatively long lengths (several tens of cm), the induction heat station was set on a motorized bench allowing the displacement of the induction coil, and therefore of the hot area, along the substrate. Although the study presented here was conducted without any displacement of the hot area, the travelling speed can range from 0.25 to 5 cm/min.

The surface temperature (T) of the graphite substrate (in the cold-wall configuration) or the graphite shell outer surface (in the hot-wall geometry) was monitored in situ during the CVD process with a high-resolution dichromatic pyrometer (Impac ISQ 5).

Deposition conditions

For all the experiments, the reactor was operated at atmospheric pressure, while the temperature and total gas flow Q_{tot} ranged from 1000 to 1100°C and from 200 to 850 sccm (standard $\text{cm}^3 \cdot \text{min}^{-1}$), respectively. A list of representative experiments is given in Table 1. Runs at higher temperatures were not carried out in the hot wall geometry due to the risk of silica substrate softening.

Deposition of the pyrolytic carbon interlayer

The first coatings deposited directly on the silica tubes showed a strong chemical bonding that resulted, on cooling, to multiple cracking. A thin layer of pyrolytic carbon (PyC) was therefore deposited at the surface of the SiO_2 tube. This interlayer was deposited in the

same reactor by injection of pure propene at low pressure ($Q_{C_3H_6} = 100$ sccm, $T = 1000^\circ\text{C}$, $P = 3$ kPa). Its anisotropic structure was found to promote the SiC/SiO₂ interface delamination.

Characterization of the coatings

The morphology of the coatings was characterized with a field emission gun scanning electron microscope (SEM) (FEI Quanta 400F).

Electron probe microanalyses (EPMA) (SX 100 from CAMECA, France) were conducted on cross-sections of CVD-coated tube fragments. The Si, C and O concentrations were assessed using the wavelength dispersive spectroscopy (WDS) mode (10 kV, 10 nA). Punctual and line scan measurements were performed along the cross section of the coatings, with a spatial resolution of approximately $1 \mu\text{m}^3$.

Raman microprobe (RM) analyses (Labram HR from Horiba Jobin Yvon) were also conducted. The excitation source was a He-Ne laser ($\lambda=632.8$ nm). The power was kept below 1 mW to avoid heating of the sample. The lateral resolution of the laser probe was close to $1 \mu\text{m}$ and the depth analyzed was less than $1 \mu\text{m}$. As for EPMA, punctual and line scan analyses were recorded along the cross section of the deposit.

Analysis of the gas phase

A semi quantitative study of the gas phase was carried out by Fourier transform spectroscopy (FTIR) at the reactor outlet (Fig. 2). The laser beam of the spectrometer (Nicolet 550) was led through a room temperature analysis cell (with two ZnSe windows at both ends) installed at the reactor outlet (absorption configuration). While the reaction chamber was set at atmospheric pressure, the pressure in the gas cell was adjusted at 1 kPa to avoid saturation of absorption peaks on the FTIR spectra. At the outlet of the gas cell, the infrared beam was focused on the HgCdTe detector placed below. The whole infrared beam path was enclosed and constantly purged with a nitrogen flow in order to limit the absorption of atmospheric compounds. A background spectrum was first recorded with a pure H₂ flow in the reactor and subtracted to the reacting gases spectrum. The apparatus allowed the acquisition of spectra in the wave-number range $650 - 4000 \text{ cm}^{-1}$, with a resolution of 1 cm^{-1} .

RESULTS AND DISCUSSION

The PyC interfacial layer deposited at low pressure before SiC (with a thickness of 350 nm) does not introduce major surface flaws in the SiC coating (Fig. 3). The EPMA and SEM measurements at opposite sides confirmed the chemical composition and thickness homogeneity of the SiC coatings deposited in the hot-wall geometry.

A number of thick SiC tubes were obtained with this APCVD process, and were successfully extracted from the silica substrate by taking advantage of the difference of thermal expansion coefficients between the silica substrate and the deposited SiC and the weak SiO₂/SiC interface provided by a PyC interlayer.

It is well known [10, 11] that one of the key parameters in the deposition of SiC is the precursor dilution ratio α :

$$\alpha = \frac{Q_{H_2}}{Q_{DCMS}} \quad (1)$$

The Si/C atomic ratio increases significantly with α (Table I). For α increasing from 0 to 12, the silicon atomic concentration in the coating varies from 54 %_{at.} to 67 %_{at.} The oxygen

concentration was found to remain lower than 2 %_{at.} in all specimens. Furthermore, a higher dilution of DCMS in H₂ results in a sharp decrease of the deposition rate. At 1025 °C, the deposition rate remains below 50 μm/h when α is higher than 4. Such a deposition rate is far too low to consider a continuous deposition process for the production of thick and long tubes within a reasonable time. The Raman Spectra (Fig. 4) show no clear crystallized SiC features (expected at 750-1000 cm⁻¹) in the deposits, but a strong band at 500cm⁻¹, typical of free silicon. The intensity of the Si band varies with α in very good agreement with the Si/C ratio. However, even for $\alpha = 0$, free silicon is still present in the coating at this temperature and the SiC phase is poorly crystallized, as shown by the very broad and weak characteristic features.

A gradual improvement of the SiC crystalline state can be noticed when the deposition temperature increases. For coatings 4, 9, 10 and 11, corresponding to deposition temperatures increasing from 1025°C to 1100°C, the emergence of two bands in the 700 – 1000 cm⁻¹ region, for the highest deposition temperatures confirms the coarsening of the SiC phase (Fig. 5). In parallel, the narrow peak at 520 cm⁻¹ corresponding to crystallized silicon disappears as well as the surrounding bump due to amorphous Si. The Si/C atomic ratios obtained by EPMA are very consistent with the Raman analyses. It is worthy of note that a Si concentration of 49 %_{at.} is obtained at 1100 °C, indicating that pure SiC can be deposited in these conditions, without any additional carbon source in the gas phase.

Only few changes of the deposition rate can be noticed with the variation of temperature. The deposition process is apparently not thermally activated, suggesting a mass transfer limited regime [12]. However, since the temperature increase probably results in parallel in important changes of the gas phase composition in the hot area, the assumption of a precursor supply limitation should be considered with care.

The influence of the total gas flow rate (Q_{tot}) was also examined (see deposits 4, 7 and 8 in Table I, obtained at $Q_{tot} = 425$ sccm, 850 sccm and 213 sccm, respectively). The gas velocity is an important parameter especially in the case of a mass transfer regime where the deposit morphology can be very sensitive to the gas flow around the substrate. In addition, Q_{tot} may affect the decomposition rate of precursors through the residence time varying along the position in the hot area. At low flow rates ($Q_8 < Q_4 < Q_7$, see Table 1), the carbon concentration, as measured by EPMA, tends to increase (from 25 %_{at.} to 52 %_{at.}). These results are consistent with the Raman analyses (Fig. 6) showing that the peak assigned to crystalline Si tends to disappear at low Q_{tot} while simultaneously, the SiC characteristic bands gradually appear. The deposition rate increases significantly with Q_{tot} from 33 μm/h at 213 sccm to 237 μm/h at 850 sccm. This behavior is consistent with the previous study on the influence of temperature. The increase of the deposition rate with Q_{tot} is indeed indicative of a regime limited by diffusion. In parallel, the change in the composition of the deposit suggests a major effect of the maturation of gas phase, i.e. of the decomposition rate of DCMS into various intermediates, which may act as effective precursors of Si and C for the coating.

A minimal deposition temperature appears necessary to form a near stoichiometric coating with highly crystalline SiC in the reactor. Whereas there are only a few studies on the CVD from DCMS/H₂ [10, 13,14], several articles on the dichlorodimethylsilane (DCDMS)/H₂ system [14-16] and an abundant work on the MTS/H₂ system [11, 17-19] can be found in the literature. Féron *et al.* used DCMS at higher temperatures and atmospheric pressure in a cold wall reactor [10]. They obtained only Si-rich coatings (C/Si at. < 0.7) at much higher deposition rates limited by chemical reactions. This suggests the occurrence of DCMS depletion in the present case, in the hot wall configuration. On the other hand, Cagliostro *et al.* used DCDMS at similar temperatures and pressure in a hot wall reactor configuration [15, 16]. They found a dependence of the deposition rate with the total flow rate for $T > 900$ °C and a strong silicon excess in the coating, decreasing along the reactor axis (i.e. while the residence time increases). A similar behavior was reported in several studies of the MTS/H₂ system in relatively similar

T and P conditions. Papasouliotis *et al.* and Huttinger *et al.* evidenced, for $T = 1000\text{ }^{\circ}\text{C}$, a decrease of the deposition rate associated with a decrease of the silicon excess along the hot zone [17,18]. The decreasing of the total flow rate also reduces the deposition rate (by increasing the residence time) [17].

Since the silica substrate cannot withstand temperatures higher than $1100\text{ }^{\circ}\text{C}$ in the hot-wall configuration, only a narrow operating temperature window is allowed. Since the deposition rate is apparently not thermally activated, the gas flow rate (or the residence time) appears as a key parameter for elaboration of long tubes.

The changes in the chemical composition of the deposit indicate an influence of the temperature on the concentration of the effective Si and C precursors brought to the deposition area. This can be explained by a change of the DCMS decomposition rate in the homogeneous (gas phase) state. To support this assumption, complementary FTIR analyses of the gas phase at the reactor outlet were performed.

A room temperature spectrum of the DCMS was recorded as a reference (Fig. 7). This spectrum shows characteristic peaks of chlorosilane products, as in previous works on DCMS [20]. A table of the vibration modes of the main species from the Si-C-Cl-H system reports the peak frequencies observed experimentally and their assignments from the literature (Table II).

The infrared spectrum of DCMS at $25\text{ }^{\circ}\text{C}$ shows the presence of a weak feature at 3010 cm^{-1} corresponding to the C-H stretching in the methyl group, a very sharp and intense peak at 2260 cm^{-1} , due to the stretching of Si-H bond, a low intensity signal corresponding to C-H wagging at 1270 cm^{-1} , and a conglomerate of intense peaks in the $900 - 650\text{ cm}^{-1}$ region, due to the stretching of Si-C and Si-Cl bonds (Table II). In a second step, an investigation of the temperature effect on the gas phase composition was carried out (Fig. 8).

Whereas the spectra remains unchanged for T ranging from $25\text{ }^{\circ}\text{C}$ to $700\text{ }^{\circ}\text{C}$, major chemical modifications appear at higher temperatures. As the analysis is carried out *ex situ* at room temperature, detected molecules are necessarily stable and some of them may result from the recombination of other unstable species (e.g. free radicals). Some part of the DCMS decomposition products can also be consumed during the SiC deposition. However, the apparition of new species at the reactor outlet gives useful information for a better understanding of the APCVD process.

As shown in Fig. 8, the decomposition of dichloromethylsilane in the reactor is accompanied by the formation of HCl, HSiCl_3 , HSi_2Cl_2 and CH_4 . SiCl_4 , another stable compound, is also expected (642 cm^{-1}). However, due to the poor sensitivity of the detector at low frequencies and to other peaks overlapping, this specie could not be followed as accurately as the others. To follow the evolution of the gas phase with temperature, the main peak areas were subsequently plotted versus T (Fig. 9)

The gradual decomposition of DCMS above 700°C (b, d, e, f, g, i) corresponds to the formation of various products in the gas phase. The apparition of methane (j, l), is progressive and tends to a plateau for the highest temperatures. The formation of trichlorosilane (HSiCl_3 , curves c and k) shows a maximum at 900°C . Its concentration decreases at higher temperatures, indicating consumption, either due to the deposition on the reactor walls, or to the formation of other reactive intermediates. SiH_2Cl_2 also shows a similar behavior, its concentration decreasing strongly down to nearly zero for temperatures above $900\text{ }^{\circ}\text{C}$ (h). Hence, the formation and consumption of chlorosilanes appears to be strongly related to the silicon incorporation in the coating.

A decomposition route of the DCMS during the APCVD process can be tentatively proposed by the analysis of the above results and the previous conclusions from the literature.

Zhang and Huttinger [18] proposed a mechanism for the deposition of SiC at near atmospheric pressure from MTS/H₂ mixture. As for MTS, the Si-C bond is probably quickly dissociated into CH₃[·] and HSiCl₂[·] in the hot zone [17-19]. This assessment was confirmed by the ab initio calculations of Allendorf et al. [26]. The Si-H bond of DCMS or HSiCl₂[·] is also probably easily broken to form eventually the reactive SiCl₂, likely the major silica source for the coating [18]. In parallel, CH₃[·] readily recombines into CH₄, which has a low surface reactivity. The chlorosilanes and SiCl₄ detected by FTIR result from the recombination of the HSiCl₂[·] and SiCl₂ radicals, in the hot zone or during the cooling. The higher reactivity of SiCl₂ compared to CH₄ is responsible for the presence of excess silicon, especially at low temperatures and high α ratios. At high temperature ($T > 1050$ °C), more reactive unsaturated hydrocarbons might be formed (FTIR analyses were not carried out at these temperatures), resulting in an increase of the deposition rate and of the carbon ratio in the coating. On the other hand, higher H₂ concentrations (higher α) promote the reduction of SiCl₂ and therefore the deposition of free silicon, while they stabilize CH₄ and prevent the deposition of C.

CONCLUSION

The present paper introduced a method to prepare long and dense monolithic SiC tubes with thick walls by APCVD. Free standing SiC tubes were obtained by deposition inside a SiO₂ tube covered with pyrocarbon. An optimization of the process was carried out by analyzing the influence of different parameters such as the precursor dilution in the injected gas mixture, the total flow rate and the deposition temperature. The increase of deposition rate with the gas flow rate, and the low thermal activation of the deposition process indicate that the process is limited by mass transfer. The modification of the gas phase itself with the different parameters leads to significant differences in the final composition of the SiC deposit.

A better understanding of the process was obtained by analyzing the gas phase at the reactor outlet by FTIR spectroscopy. The production of chlorosilanes (SiCl₄, HSiCl₃ and HSi₂Cl₂) was highlighted, along with a production of methane (CH₄) and HCl. The increase of temperature promotes the reactivity of the carbon precursors, while an important dilution inhibits them and favors the reduction of chlorosilanes, hence resulting in a Si rich deposit. The increase of the deposition rate with Q_{tot} is indicative of a regime limited by diffusion.

The elaboration of longer and thicker SiC tubes is already in progress, and the mechanical testing of the samples, for instance by C-ring tests [28] is planned.

REFERENCES

- ¹C. Lorrette, C. Sauder and L. Chaffron, "Progress in developing SiC/SiC composite materials for advanced nuclear reactors" (Paper presented at the 18th International Conference on Composite Materials, Jeju Island, Korea, 21-26 August 2011), 1-4.
- ²C. Ayranci, J. Carey, "2D braided composites: A review for stiffness critical applications", *Composite Structures* 85 (2008) 43–5
- ³R.H. Jones et al., "Recent advances in the development of SiC/SiC as a fusion structural material", *Fusion Engineering and Design*, 41 (1-4) (1998), 15-24
- ⁴E.V Dyomina et al., "Low-activation characteristics of V-alloys and SiC composites", *Journal of Nuclear Materials*, 258–263 (1998), 1784–179
- ⁵A.R Raffray et al., "Design and material issues for high performance SiC_f/SiC-based fusion power cores", *Fusion Engineering and Design*, 55 (2001), 55–95
- ⁶B. Riccardi et al., "Issues and advances in SiC_f/SiC composites development for fusion reactors", *Journal of Nuclear Materials*, 329–333 (2004), 56–65

- ⁷H. Feinroth et al., “Multi-Layered Ceramic Tube for Fuel Containment Barrier And Other Applications In Nuclear And Fossil Power Plants”, Patent WO 2006/076039, (2006)
- ⁸G. Chollon, R. Naslain et al., “High temperature properties of SiC and diamond CVD-monofilaments”, *Journal of the European Ceramic Society* 25 (2005), 1929–1942
- ⁹T.T. Cheng et al., “The microstructure of sigma 1140+SiC fibres”, *Materials Science and Engineering : A* 260 (1999), 139–145
- ¹⁰O. Féron, “In situ kinetic analysis of SiC filaments CVD”, *Diamond and Related Materials* 11 (2002), 1234–1238
- ¹¹G. Chollon, M. Placide et al., “Transient stages during the chemical vapour deposition of silicon carbide from CH₃SiCl₃/H₂: impact on the physicochemical and interfacial properties of the coatings”, *Thins Solid Films* 520 (2012), 6075-6087
- ¹²G. Astarita, “Regimes of mass transfer with chemical reaction”, *Ind. Eng. Chem.* 58, (1966), 18–26
- ¹³H. Vincent, “Chemically vapour-deposited coatings of silicon carbide on planar alumina substrates”, *J. Mater. Chem.* (1992), 567 – 574
- ¹⁴J.J. Brennan, “Interfacial studies of chemical-vapor-infiltrated ceramic matrix composites”, *Mat. Science and Eng. A*126 (1990), 203 – 223
- ¹⁵D.E. Cagliostro and S.R. Riccitiello, “Model for the formation of silicon carbide from the pyrolysis of dichlorodimethylsilane in hydrogen”, *J. Am. Ceram. Soc.* 76 (1993), 39 – 53
- ¹⁶D.E. Cagliostro and S.R. Riccitiello, “Comparison of the pyrolysis products of dichlorodimethylsilane in the chemical vapor deposition of silicon carbide on silica in hydrogen or argon”, *J. Am. Ceram. Soc.* 77 (1994), 2721 – 2726
- ¹⁷Papasouliotis et al., “Experimental study of atmospheric pressure chemical vapor deposition of silicon carbide from methyltrichlorosilane”, *J. of Mat. Res.* 14 (1999), 3397 – 3409
- ¹⁸W. Zhang and K. Hüttinger, “CVD of SiC from Methyltrichlorosilane”, *Chem. Vap. Deposition* 7 (2001), 167 – 181
- ¹⁹F. Loumagne, F. Langlais and R. Naslain, “Reaction mechanisms of the chemical vapor deposition of SiC-based ceramics from CH₃SiCl₃/H₂ gas precursor”, *J. Crystal Growth* 155 (1995), 205 – 213
- ²⁰O. Féron, “Filament CVD de SiC de composition et microstructure adaptées au procédé Snecma d’enduction par le titane liquide”, (Internal report presented during postdoctoral position, Bordeaux, December 2000)
- ²¹S. Jonas et al., “FTIR In Situ Studies of the Gas Phase Reactions in Chemical Vapor Deposition of SiC”, *Journal of Electrochemical Society*, 142 (1995), 2357-2362
- ²²J. N. Burgess and T. J. Lewis, “Kinetics of the Reduction of Methyltrichlorosilane by Hydrogen,” *Chem. Ind.*, 976–77, 1974
- ²³V. Hopfe et al., “In-Situ FTIR Emission Spectroscopy in a Technological Environment : Chemical Vapour Deposition (CVD) of SiC Composites”, *Journal of Molecular Structure* 347 (1995), 331-342
- ²⁴G. Socrates, “Infrared Characteristic Group Frequencies” (1980)
- ²⁵Brennfleck et al., “In-Situ spectroscopic monitoring for SiC-CVD process control”, *Phys. IV* 9, (2009), 1041 – 1048
- ²⁶W. M.D. Allendorf and C.F. Melius, “Theoretical study of the thermochemistry of molecules in the Si-C-Cl-H system”, *J. Phys. Chem.* 97 (1993), 720 – 728
- ²⁷T.D. Gulden, “Deposition and microstructure of vapor-deposited silicon carbide”, *Journal of the American Ceramic Society* 51, Issue 8 (1968) 424 – 428
- ²⁸ASTM G38 - 01(2007) Standard Practice for Making and Using C-Ring Stress-Corrosion Test Specimens

TABLES

Table I. Deposition conditions for the CVD of SiC

N°	Q _{tot} (sccm)	$\alpha = Q_{H_2}/Q_{DCMS}$	T (°C)	Si % _{at.}	Deposition rate (μm/h)
1	425	0	1025	54	124
2	425	1	1025	55	216
3	425	2	1025	72	296
4	425	4	1025	61	69
5	425	8	1025	67	50
6	425	12	1025	65	39
7	850	4	1025	76	237
8	213	4	1025	48	33
9	425	4	1050	57	70
10	425	4	1075	53	60
11	425	4	1100	49	72

Table II. Peak frequencies observed experimentally and assignments from literature:
Si-H-C-Cl

Observed peak position (cm ⁻¹)	Vibration mode	Chemical compound	Literature values
590	Si-Cl stretching	SiCl ₃ or Si ₂ Cl ₆	585, 592 [23]
620		SiCl ₄	619 [23], 620 [21]
642		SiCl ₄	641 [23]
756		DCMS	752, 762 [23]
807		HSiCl ₃	805 [24]
848	Si-C stretching	DCMS	[20]
860			[21]
884			[25]
893			
949	Si-Cl stretching	SiH ₂ Cl ₂	960 [22]
1270	C-H wagging	DCMS	1270 [23] 1272 [21]
1307		CH ₄	1305 [21] 1306 [23] 1310 [22]
2217	Si-H stretching	DCMS	2220 [24]
2260		HSiCl ₃	SiH _n Cl _{4-n} : 2248, 2260 [21] 2270 [22]
2970	C-H stretching	DCMS	-
3010		CH ₄	3018 [22]
2700-300	H-Cl stretching	HCl	2500-3095 [22]

FIGURES

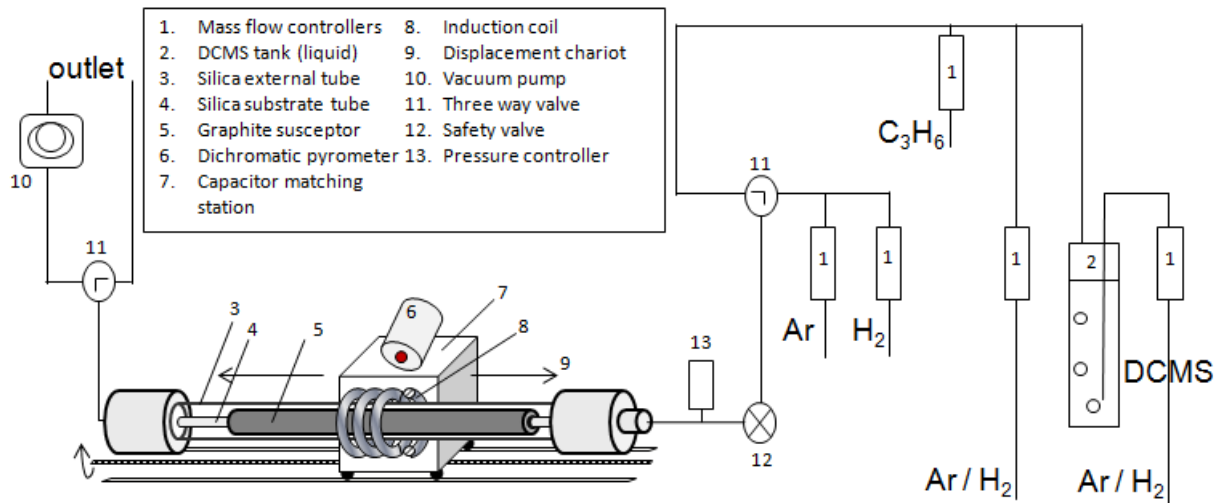


Figure 1. APCVD reactor for SiC deposition

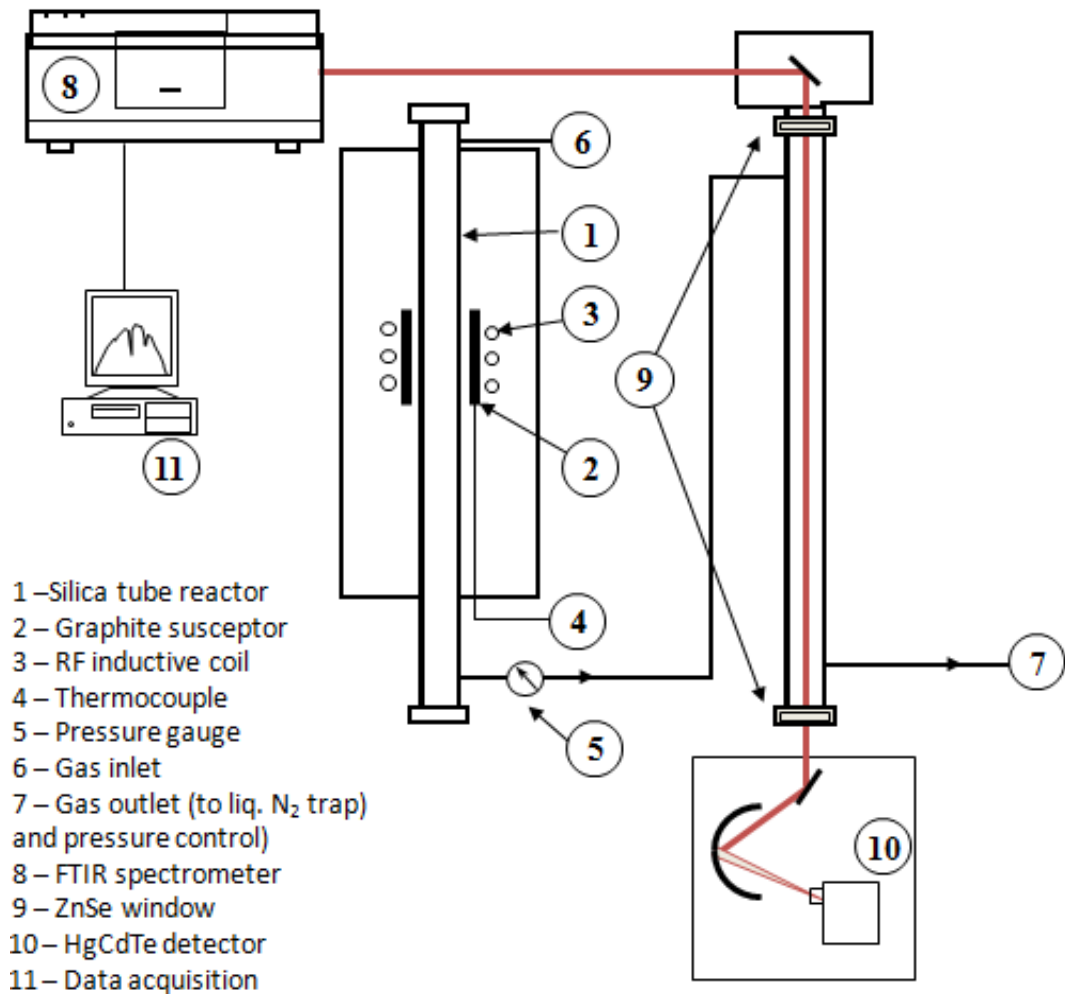


Figure 2. Experimental setup for deposition and FTIR analysis of the gas phase

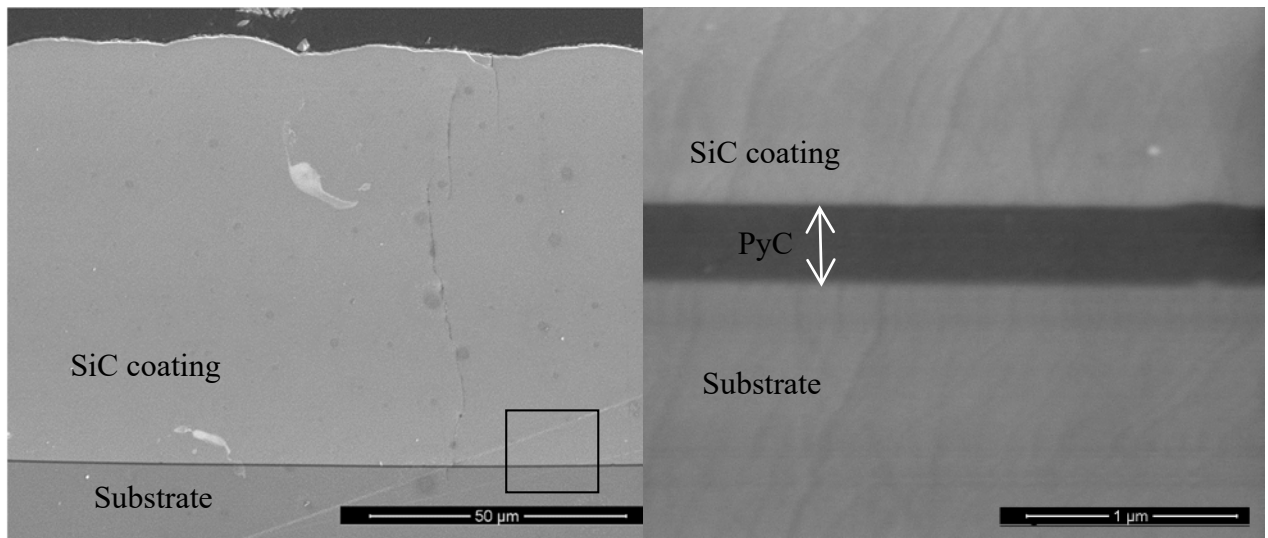


Figure 3. Cross section of the $\text{SiO}_2/\text{PyC}/\text{SiC}$ interfacial region

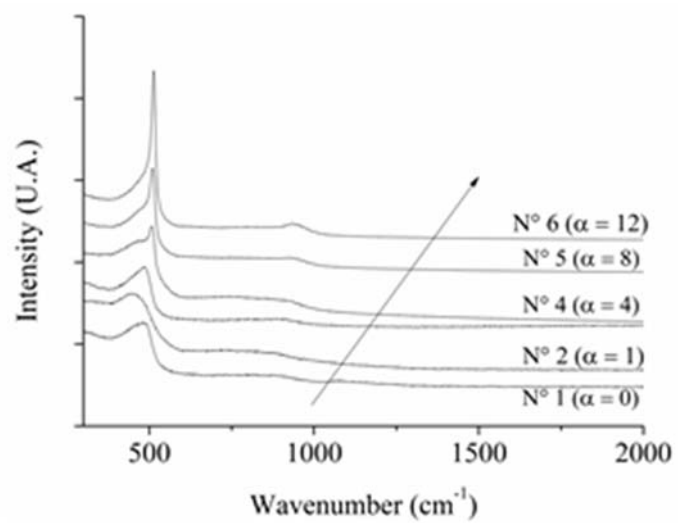


Figure 4. Influence of α on the Raman spectra

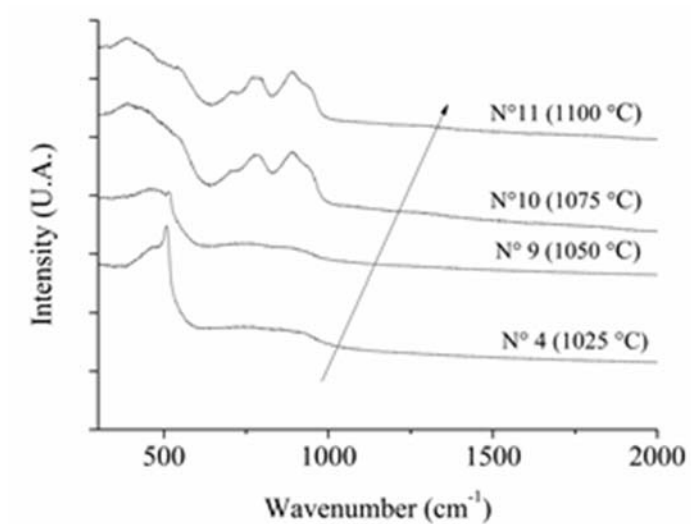


Figure 5. Influence of the temperature on the Raman spectra

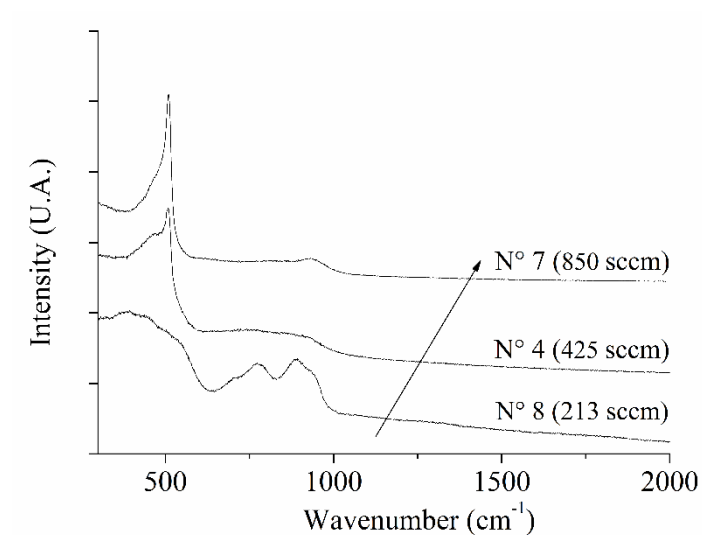


Figure 6. Influence of the total flow rate on the Raman spectra

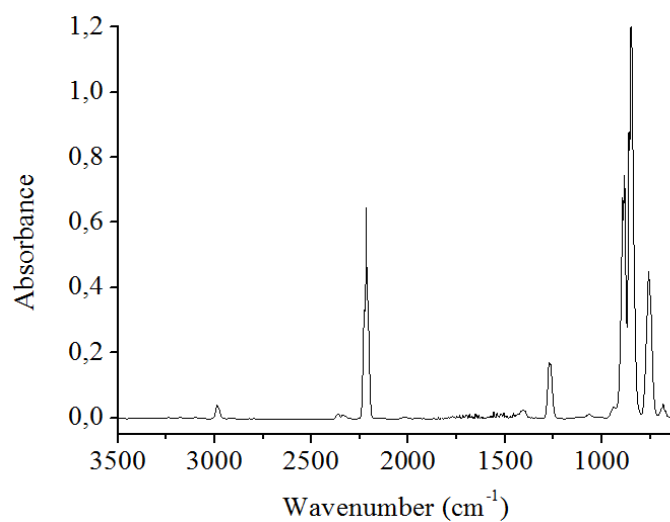


Figure 7. FTIR spectrum of DCMS at room temperature (650-3500 cm^{-1})

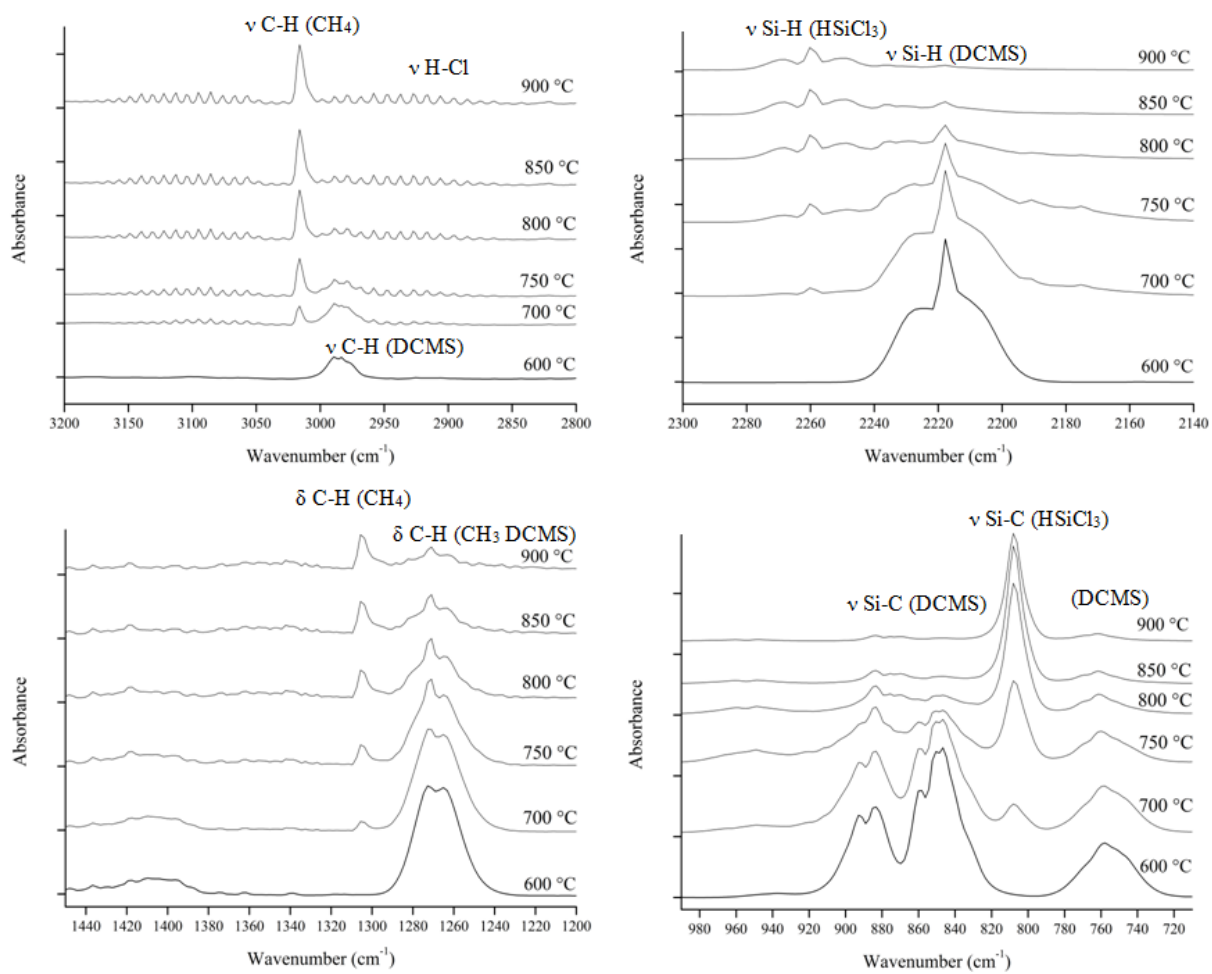


Figure 8. Evolutions of FTIR spectra of DCMS with temperature

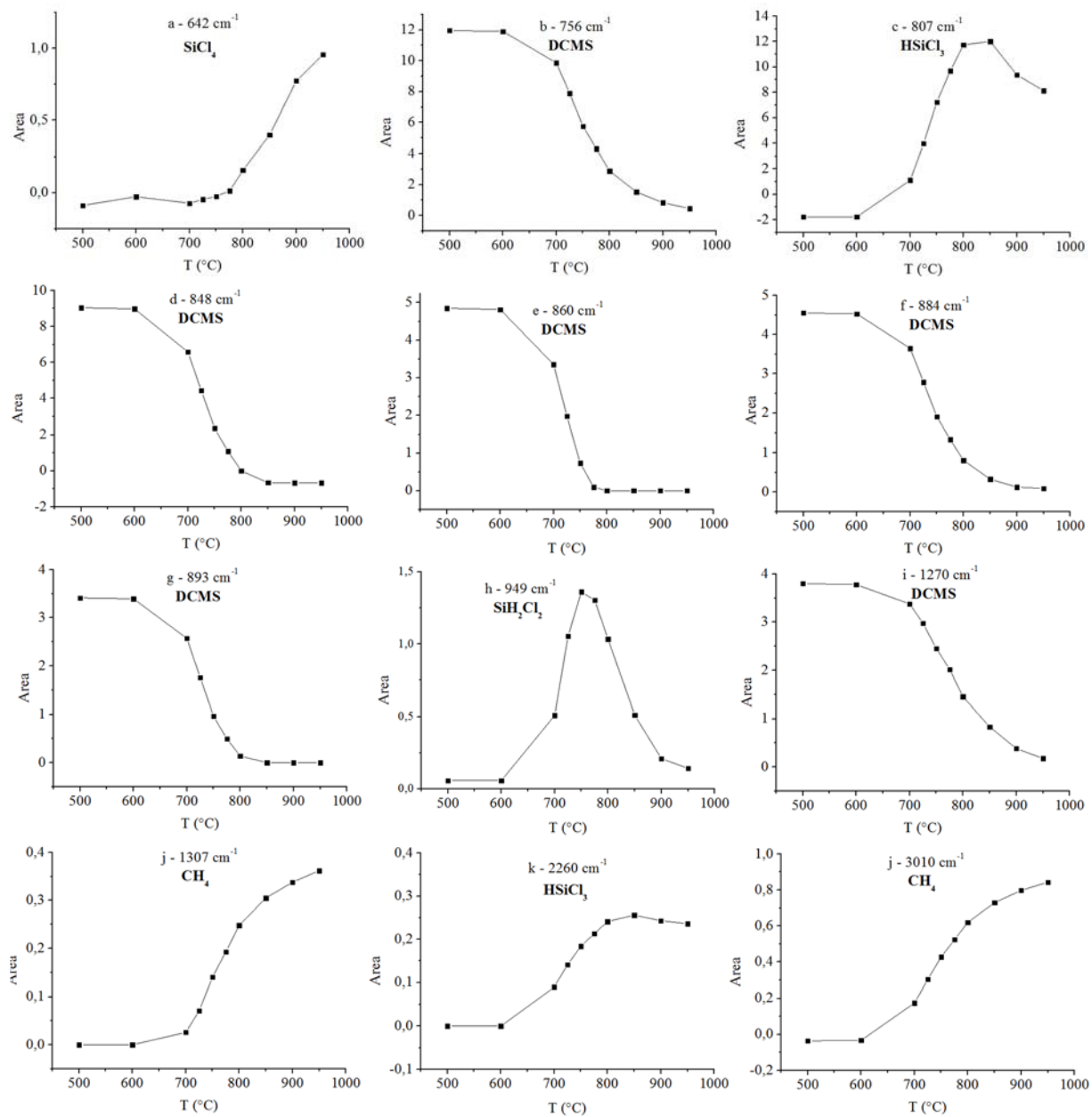


Figure 9. Peak areas of the main FTIR features (a...l) versus temperature